Influence of mechanically alloyed fraction and hot rolling temperature in the last pass on the structure of Fe-14Mn-6Si-9Cr-5Ni (mass. %) shape memory alloys processed by powder metallurgy

B. PRICOP[a], B. ÖZKAL[b], U. SÖYLER[b], J. VAN HUMBEECK[c], N. M. LOHAN[a], M. G. SURU[a], L.-G. BUJOREANU[a,*]
[a]*Faculty of Materials Science and Engineering, The "Gheorghe Asachi" Technical University of Iaşi, Bd. D. Mangeron 67, 700050 Iaşi, Romania*
[b]*Particulate Materials Laboratory, Metallurgical and Materials Engineering Department, Istanbul Technical University, 34469 Maslak, Istanbul, Turkey*
[c]*Department of Metallurgy and Materials Engineering, Katholieke Universiteit Leuven, BE-3001 Leuven Belgium*

Samples of Fe-14Mn-6Si-9Cr-5Ni (mass. %) shape memory alloy were sintered from two powder mixtures: (i) as blended (0_MA) and (ii) equal amounts of as blended and mechanically alloyed (MA'd) powders (50_MA). In order to increase the compactness degree, different specimens were hot rolled at 1373 K and the last rolling pass was performed at four different temperatures: (i) room temperature (RT); (ii) 873 K; (iii) 1073 K and (iv) 1373 K. In order to emphasize the influence of both MA'd fraction and rolling final temperature, the eight resulting specimens were analysed by X-ray diffraction (XRD) as well as by scanning electron microscopy (SEM). XRD results allowed the qualitative and quantitative identification of the three component phases, namely γ (face centred cubic, fcc)-parent phase, ε-(hexagonal close packed, hcp) martensite and α'-(body centred tetragonal, bct) martensite. SEM micrographs enabled to observe the influence of MA'd fraction on the relative amounts of the three phases. The results suggest that the presence of MA'd fraction contributes to destabilization of α'(bct) martensite and increase of the amount of ε(hcp) martensite, with favourable effects on shape memory behaviour.

(Received January 27, 2014; accepted March 13, 2014)

Keywords: Mechanical alloying, Powder metallurgy, Fe-Mn-Si-Cr-Ni shape memory alloys, XRD, SEM

1. Introduction

Shape memory alloys (SMAs) are smart materials able to recover from being deformed when heated [1]. Presently there are five major types of commercial SMA systems, based on: (i) NiTi; (ii) CuZnAl; (iii) CuAlNi; (iv) FeNiCoTi and (v) FeMnSi [2]. Due to their relatively cheap cost, FeMnSi SMAs have high application potential and, to date, two alloys became commercially available, Fe-28 Mn-6 Si-5 Cr [3] and Fe-14 Mn-5 Si-9 Cr-5 Ni [4] (mass. %, as all compositions will be listed hereinafter).

In FeMnSi SMAs the governing mechanism of shape memory effect (SME) behaviour relays on stress induced formation of ε (hexagonal close packed, hcp) martensite and on its thermally induced reversion to γ (face centre cubic, fcc) austenite, on heating [5]. At low Mn content or at high deformation degrees, besides ε hcp, α' (body centre tetragonal, bct) martensite can be additionally stress induced [6].

Classical metallurgy processing of FeMnSi SMAs, consisting in induction melting and casting under protective atmosphere, has several drawbacks, caused by difficult Si incorporation into melt, Mn loss on melting, high cracking rate on cooling and time-consuming chemical composition homogenization. These arguments suggest that a solid-state processing route, such as powder metallurgy (PM) could be used to produce accurate-composition alloys, while the association with mechanical alloying (MA), has the potential to increase compactness and to contribute to grain size controlling, thus avoiding most of aforementioned drawbacks of classical metallurgy.

Unlike other SMA systems, such as Ti-Ni, Cu-Zn-Al or Cu-Al-Ni, which were developed both by classical metallurgy (ingot melting, alloying and casting) and by PM, Fe-Mn-Si-based alloys have been mostly characterized under classical metallurgy-processed form. Promising results were reported by a part of the present authors, on thermally induced reversion of stress induced martensite [7, 8, 9, 10], and on its formation during mechanical cycling [11] in PM FeMnSiCrNi alloys. On the other hand, promising results were recently reported on the advantages of using MA and subsequent sintering in the production of the Fe–Mn–Si SMAs with better mechanical properties [12]. Based on above mentioned state of the art, the present paper aims to report the effects of correlating PM-MA processing with a hot working technique meant to increase compactness, such as rolling [13], while discussing the structural changes caused by the variation of temperature in final rolling step [14] in a PM Fe-14Mn-6Si-9Cr-5Ni SMA.

2. Materials and methods

Powder mixtures with nominal chemical composition Fe-14Mn-6Si-9Cr-4Ni (mass %) were sintered from two powder compacts: (i) as blended (0_MA) and (ii) equal amounts of as blended and mechanically alloyed (50_MA) [15]. The powder aggregates were pressed and sintered at 1390 K, under cracked ammonia [16] and hot rolled at 1373 K [17] with the last rolling pass performed at four different temperatures: (i) room temperature (RT); (ii) 873 K; (iii) 1073 K and (iv) 1373 K. It was assumed that this processing route has the potential to produce a larger fraction of martensite compared to samples in the as-austenitized condition [18]. The eight resulting samples were analysed by X-ray diffraction (XRD) and scanning electron microscopy (SEM).

XRD evaluation was performed with a Seifert 3003 TT goniometer with 2θ ranging from 40 to100°, the scanning was step by step, the size of the step was 0,02° and the time allocated for each step was 2s. SEM observations were performed by means of a FEI Quanta SEM-FIB 200 3D dual beam microscope, under protective atmosphere.

3. Results and discussion

The XRD results are summarized in Fig. 1, for 0_MA and Fig. 2 for 50_MA. Each of the figures comprises four XRD patterns corresponding to room (RT) as well as to the three temperatures of final rolling pass: 873K, 1073K and 1373K.

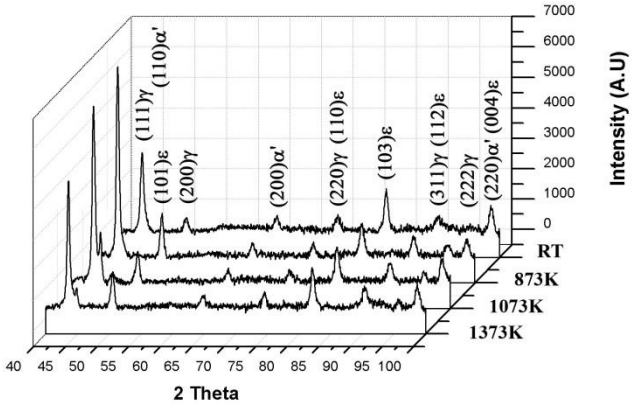

Fig. 1. XRD patterns of 0_MA samples, hot rolled at 1373 K with the last rolling pass performed at four different temperatures: room temperature (RT), 873K, 1073K and 1373K.

Using 00-034-0396, 01-071-8285 and 01-071-8288 XRD databases, the characteristic diffraction peaks were identified being ascribed to the three main component phases, γ face centred cubic (fcc) – parent phase (austenite), ε hexagonal close-packed (hcp) – martensite and α' body centre tetragonal (bct) – martensite.

Fig. 1 displays the XRD patterns characteristic to 0_MA specimens, within the significant region of 2Θ angle between 40 and 100°.

It is noticeable that after the last rolling pass performed at RT the XRD pattern, displayed in the last plane, contains a large amount of ε hcp-martensite represented by the variant (103). The presence of ε hcp-martensite, which has been directly associated with the possibility to obtain recoverable strains by SME [19] has been ascertained by the occurrence of several diffraction peaks which can be ascribed to this phase. For instance, the main diffraction peak (101) of this phase was noticed at the sample with the last rolling pass performed at 1073K.

The structure also contains a large amount of γ fcc-austenite identified by its main diffraction peak, (111), located at 2Θ=43.45°. The presence of austenite is confirmed by several diffraction maxima, such as (200), (220) and probably (311). These four orientations represent the main crystallographic variants of this phase.

Due to the rather low amount of Mn (14 mass %) the presence of α' bct-martensite can be also expected [20] being represented mostly by its secondary diffraction peak (200). With increasing the temperature of final rolling pass, the intensity of major diffraction maxima increases and several of them, which were overlapping at RT, become distinctly noticeable, such as the main diffraction maximum of α' bct-martensite, (110).

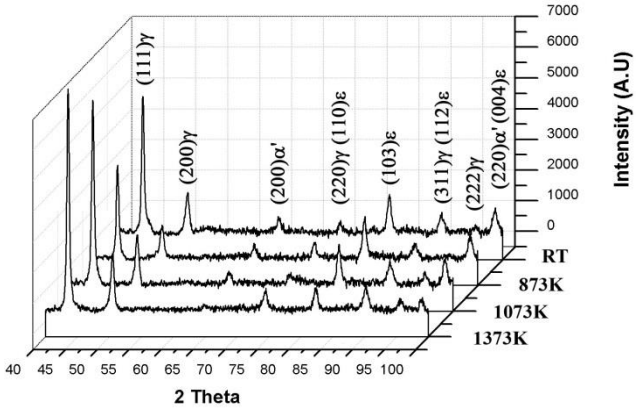

Fig. 2. XRD patterns of 50_MA samples, hot rolled at 1373 K with the last rolling pass performed at four different temperatures: room temperature (RT), 873K, 1073K and 1373K

Fig. 2 displays the XRD patterns characteristic to 50_MA specimens, within the significant region of 2Θ angle between 40 and 100°. It can be seen that in this samples, which contain equal amounts of as blended and mechanically alloyed powders, the main diffraction maximum of α' bct-martensite (110) no longer appears at all, instead one of its secondary diffraction maxima (200) reaches a maximum intensity at 873K. The occurrence of ε hcp-martensite was established by the presence of several secondary diffraction peaks that reached a maximum of intensity in the sample with the last rolling pass performed at 873K.

Since most of the diffraction maxima of the three phases are overlapping within the significant region of 2Θ=40–100°, in this study only the intensities of the non-superimposed peaks for each of the three phases were considered for performing a relative semi-quantitative evaluation [21]. Thus the relative amount of γ-fcc was considered to be proportional with the intensities of γ_{111} + γ_{200} + γ_{222} peaks, the amount of ε-hcp with ε_{101} + ε_{103} and the amount of α'-bct with α'_{200} + α'_{110}. The obtained results are presented in Table 1.

Table 1. XRD semi-quantitative evaluation of the relative amounts of the three phases (γ fcc-austenite, ε hcp-martensite and α' bct-martensite) (%).

Sample type	γ	ε	α'
0_MA_RT	67.8	31.1	1.1
0_MA_873K	84.8	14.6	0.6
0_MA_1073K	64.2	18.5	17.3
0_MA_1373K	69.1	18.8	12.1
50_MA_RT	79.6	19.6	0.8
50_MA_873K	73.3	25.7	1.0
50_MA_1073K	82.9	16.4	0.7
50_MA_1373K	89.5	9.9	0.6

As noticeable, the samples 50_MA presented low relative amounts, up to 1 %, of α' bct-martensite, while 0_MA reached as much as 17.3% α' in specimen 0_MA_1073K.

Although a relatively large amount, 18.5 %, of ε hcp-martensite was obtained in this sample, the highest percentage of this phase, 31.1 %, was achieved in sample 0_MA rolled at RT while the minimum, 9.9 %, was found in 50_MA hot rolled at 1373K.

The γ fcc-austenite presented a minimum of 64.2% in 0_MA rolled at 1073K and a maximum of 89.5 % in 50_MA hot rolled at 1373K. Overall, the average amounts of 20.8% ε hcp-martensite and 7.8% α' bct-martensite were obtained within the 0_MA samples while the 50_MA samples presented only 17.9% ε hcp-martensite and 0.8% α' martensite. Considering the present results, one can assume that the 0_MA samples, based on the higher percentage of ε hcp-martensite, will have better shape memory effect (SME) in regards with the lower percentage of the same phase obtained in 50_MA samples. Although 0_MA samples presented higher percentage of ε hcp-martensite, they also had higher percentage of α' bct-martensite, which is known to impede the backward motion of the Shockley partial dislocations and thus diminishing the shape memory effect [22]. While 50_MA samples had a lower overall average percentage of ε hcp-martensite, only 17,9%, they also had a significantly lower quantity of α' bct-martensite (0,8%) which will lead to a higher SME [23].

Figs. 3 and 4 present the SEM micrographs of the samples with highest amounts of ε hcp-martensite, namely 0_MA rolled at RT, with 31.1 % and 50_MA rolled at 873K, with 25.7 %, respectively.

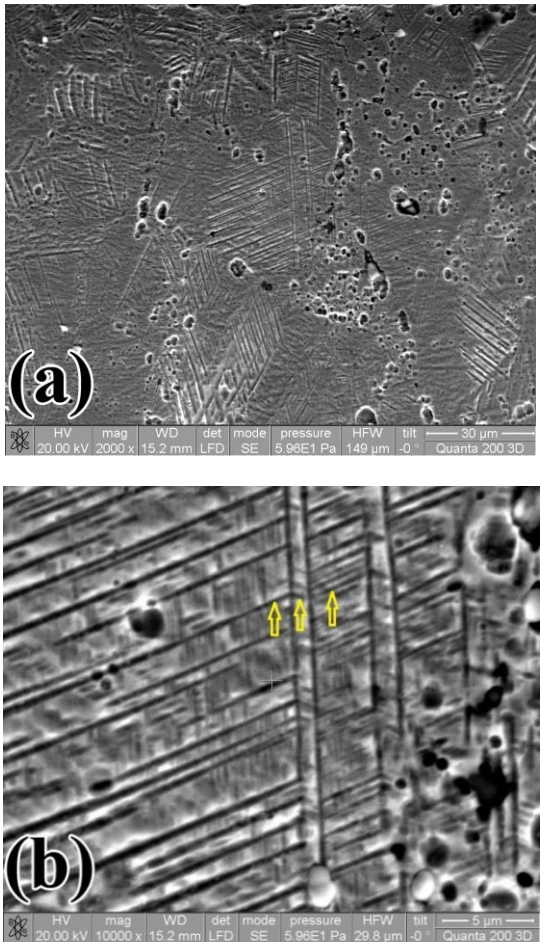

Fig. 3. SEM micrographs of 0_MA sample, hot rolled at 1373 K with the last rolling pass performed at RT: (a) general aspect; (b) detail of martensite plates intersecting two annealing twins

Fig. 3 presents the SEM micrograph of 0_MA sample rolled at RT, which has the highest percentage of ε hcp-martensite. In Fig. 3(a) the morphology of ε hcp-martensite can be clearly seen. A magnified micrograph of Fig. 3(a) is presented in (b), which presents tilted primary plates of ε hcp-martensite, up to 50 µm in length, and two annealed twins. The plates belong mostly to a single crystallographic variant of martensite, symmetrically oriented in regards of the twinning plane [24]. Moreover, some of ε hcp-martensite plates remained continuous, after intersecting the twin boundary, as in the example illustrated by arrows in Fig. 3(b).

Fig. 4 presents the SEM micrograph of 50_MA sample rolled at 873K, which had the second largest amount, 25.7 %, of ε hcp-martensite. It seems that the presence of mechanically alloyed powder from this sample, coupled with hot rolling at 873K, caused the occurrence of a very fine matrix of ε hcp-martensite, which is beneficial for SME enhancement [25]. It can be assumed that the destabilization of α' bct-martensite, which plays a similar role with stacking faults in the

formation of ε hcp-martensite in a domain-specific manner [26], when coupled with the presence of fine plates of ε hcp-martensite, has the potential to contribute to obtaining the highest SME of all samples.

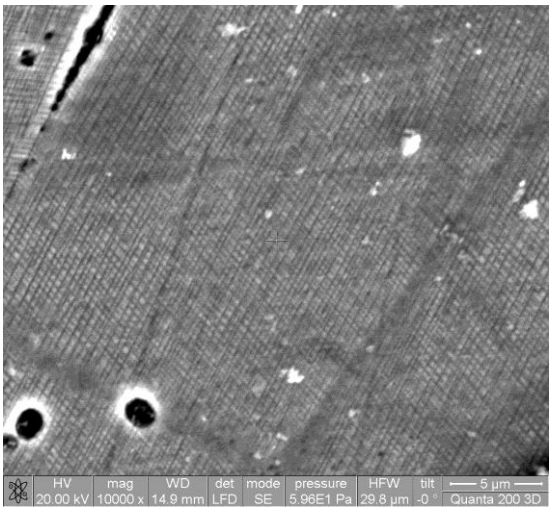

Fig. 4. SEM micrograph of 50_MA sample, hot rolled at 1373 K with the last rolling pass performed at 873K.

4. Summary and conclusions

Samples of Fe-14Mn-6Si-9Cr-5Ni (mass. %) SMA, sintered from two powder mixtures (i) as blended (0_MA) and (ii) equal amounts of as blended and mechanically alloyed powders (50_MA), were hot rolled at 1373 K and the last rolling pass was performed at four different temperatures: (i) room temperature (RT); (ii) 873 K; (iii) 1073 K and (iv) 1373 K. The eight resulting samples were then analysed by scanning electron microscopy and X-ray diffraction.

The XRD analyses showed that the highest percentage of ε hcp-martensite (31.1%) was obtained in 0_MA sample with final rolling pass performed at RT. Although 0_MA samples presented higher percentages (an average of 20.8 %) of ε hcp-martensite, they also had elevated amounts (an average of 7.8 %) of α' bct-martensite, which is detrimental to SME. The best (finest) ε hcp-martensite matrix was obtained in 50_MA sample rolled at 873K. The presence of MA'd fraction contributed to the destabilization of α' bct-martensite, thus increasing the possibility of obtaining higher SME. Since thermal memory behaviour, in Fe-Mn-Si SMAs, requires the presence of ε hcp-martensite, it can be assumed that MA'd fraction enhances shape memory behaviour.

Acknowledgements

This research work was supported by the project PN-II-ID-PCE-2012-4-0033, contract 13/ 2013.

One of the authors, Bogdan Pricop acknowledges the KULeuven for his three months research stay at the department of Metallurgy and Materials Engineering.

References

[1] J. Ma, I. Karaman, Science **327**, 1468 (2010).
[2] L. Sun, W. M. Huang, Z. Ding, Y. Zhao, C. C. Wang, H. Purnawali, C. Tang, Mater Design **33**, 577 (2012).
[3] H. Otsuka, H. Yamada, T. Maruyama, H. Tanahashi, S. Matsuda, M. Murakami, ISIJ Int, **30**, 674 (1990).
[4] Y. Moriya, H. Kimura, S. Ishizaki, S. Hashizume, S. Suzuki, H. Suzuki, T. Sampei, J. Phys. **III(**1), 433 (1991).
[5] T. Maki, K. Otsuka, C. M. Wayman (Eds.), Cambridge, University Press, p. 117, 1998.
[6] L. Bracke, G. Mertens, J. Penning, B. C. De Cooman, M. Liebeherr, N. Akdut, Metall Mater Trans A **37A**, 307 (2006).
[7] L. G. Bujoreanu, S. Stanciu, B. Özkal, R. I. Comăneci, M. Meyer, ESOMAT 2009, 05003 (2009).
[8] B. Pricop, U. Söyler, N. M. Lohan, B. Özkal, L. G. Bujoreanu, D. Chicet, C. Munteanu, J Mater Eng Perform, **21**, 2407 (2012).
[9] B. Pricop, U. Söyler, B. Özkal, N. M. Lohan, A. L. Paraschiv, M. G. Suru, L. G. Bujoreanu, Materials Science Forum, **738-739**, 237 (2013).
[10] B. Pricop, U. Söyler, N. M. Lohan, B. Özkal, D. Chicet, A. David, L.-G. Bujoreanu, Optoelectron and Adv. Mater – Rapid Commun **5(**5), 555 (2011).
[11] B. Pricop, U. Söyler, R. I. Comăneci, B. Özkal, L. G. Bujoreanu, Physics Procedia **10**, 125 (2010).
[12] T. Saito, C. Kapusta, A. Takasaki, Mat Sci Eng A **592**, 88 (2014).
[13] G. J. Arruda, V. T. L. Buono, M. S. Andrade, Mat Sci Eng, A **273–275**, 528 (1999).
[14] A. Baruj, T. Kikuchi, S. Kajiwara, N. Shinya, Mat Sci Eng, A **378**, 333 (2004).
[15] A. U. Söyler, B. Özkal, L. G. Bujoreanu, TMS Suppl Proc., **1**, 577 (2011).
[16] A. U. Söyler, B. Özkal, L. G. Bujoreanu, TMS Suppl. Proc., **3,** 785 (2010).
[17] L. G. Bujoreanu, V. Dia, S. Stanciu, M. Susan, C. Baciu, Eur. Phys. J. Special Topics, **158**, 15 (2008).
[18] N. Stanford, D. P. Dunne, Mat Sci Eng, A **422**, 352 (2006).
[19] Q. Gu, J. Van Humbeeck, L. Delaey, Scripta Metall Mater, **30**(12), 1587 (1994).
[20] B. Dubois, Trait Thermique, **234**, 27 (1990).
[21] T. Sawaguchi, L. G. Bujoreanu, T. Kikuchi, K. Ogawa, F. Yin, ISIJ Int, **48**(1), 99 (2008).
[22] S. Kajiwara, Mat Sci Eng, A **273–275**, 67 (1999).
[23] X. H. Min, T. Sawaguchi, X. Zhang, K. Tsuzaki, Scripta Mater, **67**, 37 (2012).
[24] T. Sawaguchi, L. G. Bujoreanu, T. Kikuchi, K. Ogawa, M. Koyama, M. Murakami, Scripta Mater, **59**, 826 (2008).
[25] D. Dunne, Diffusionless transformations, high strength steels, modelling and advanced analytical techniques, **2**, E Pereloma, D V Edmonds (Eds), Woodhead Publishing, p. 83 (2012).
[26] H. B. Peng, Y. H. Wen, G. Liu, C. P. Wang, N. Li, Adv Eng Mater **13(**5), 388 (2011).

*Corresponding author: lgbujor@yahoo.com